
Thallium-201 SPECT Increases Detectability of Thyroid Cancer Metastases

N. David Charkes, Richard A. Vitti, and Kevin Brooks

Section of Nuclear Medicine, Department of Diagnostic Imaging, Temple University Hospital, Philadelphia, Pennsylvania

Thallium-201- (^{201}Tl) chloride is known to accumulate in metastatic foci of differentiated thyroid carcinoma, but small and deep-seated lesions are generally not detectable by planar imaging. We have evaluated the use of ^{201}Tl -chloride single-photon emission computed tomography (SPECT) in 41 post-thyroidectomy patients with differentiated thyroid carcinoma and one with medullary carcinoma; planar imaging alone was done in eight additional patients (total 50). Of 20 patients with known metastatic disease, planar ^{201}Tl images were positive in 12 (60%) but SPECT revealed an additional 5 (25%) who had metastases (total 85%). SPECT revealed foci as small as 1.0 cm in the neck and 1.5 cm in the lungs, and was particularly useful in detection of disseminated micronodular pulmonary metastases, especially in patients whose scans were negative with diagnostic doses of ^{131}I . Some pitfalls in interpretation of the tomographic reconstructions were found. Thallium-201 SPECT is a marked improvement over planar imaging in the detection of metastases of differentiated thyroid cancer.

J Nucl Med 1990; 31:147-153

Thallium-201-chloride has been found to accumulate in 90%–100% of primary thyroid cancers, in large series (1–7), and in many metastatic deposits as well. In patient groups of ten or more, the detectability of metastatic lesions has ranged from 35% to 91% (5,6,8–11). In regional neck nodes, positive ^{201}Tl uptake has been associated with palpable adenopathy (1,5,8,12) or size >1.5 cm (6,9,13,14), and false-negative uptake with cystic lesions (15) or impalpable, deeply placed nodes <1.0 cm (5,9,13,14). Distant (lung, bone) metastases have been seen by ^{201}Tl -chloride only in patients with roentgenographically visible nodules (8,16), generally >2.0 cm (9). Recommendations concerning the use of ^{201}Tl -chloride in the management of postoperative thy-

roid cancer patients have ranged from enthusiastic (6, 10,17) to cautious (8,11).

Thallium-201 decays by electron capture to Hg-201, emitting x-rays of 69–80 keV in 94.4% of decays. These photons are highly attenuated in bodily tissues. It occurred to us that detectability of metastatic lesions by ^{201}Tl -chloride might be increased by the use of single photon emission computed tomography (SPECT). Accordingly, we prospectively investigated a group of 49 postoperative patients with differentiated thyroid cancer and one with medullary carcinoma, for the presence of metastatic disease with ^{201}Tl -chloride. We found that SPECT significantly improved the ability of this tracer to detect regional and distant disease.

MATERIALS AND METHODS

We studied 49 patients who had undergone total or near-total thyroidectomy for differentiated thyroid cancer (papillary or follicular carcinoma), and one patient with medullary carcinoma (total 50). All patients except two had previously been evaluated by iodine-131 (^{131}I) scans of the neck and chest, and by serum thyroglobulin determinations. In addition, 12 had computerized tomography (CT) study of the neck and chest, and one subsequently came to post mortem examination.

The presence of metastatic disease was established in 20 patients by surgical pathology (14 patients), ^{131}I scanning (12 patients), chest roentgenogram (7 patients), CT (6 patients), or a combination of these methods. Each patient was injected with 2.0–2.5 mCi ^{201}Tl - (thallous) chloride, and planar images were made of the neck and chest beginning 20 min postdose, using the G.E. Starcam gamma camera system (GE Medical Systems, Milwaukee, WI) with LEAP collimator and a 20% symmetric window centered over the 72-keV photopeak. In 42 patients, SPECT imaging was performed by acquiring data in a 64×64 word matrix at 6-degree increments for 10 sec per position along an elliptical orbit. A standard 9-point smoothing filter was applied to each of the images prior to generating transaxial, sagittal, and coronal reconstructions. Image enhancement was performed by manual adjustment of brightness and contrast on a modified exponential gray scale display. To avoid downscatter, all ^{201}Tl studies were done prior to ^{131}I imaging. The study was approved by the Temple University Research Review Committee and Medical Radiation Subcommittee, and signed informed consent was obtained from every patient.

Received Apr. 20, 1989; revision accepted Oct. 5, 1989.
For reprints contact: N. David Charkes, MD, Dept. of Diagnostic Imaging, Temple University Hospital, 3401 N. Broad St, Philadelphia, PA 19140.
Presented in part at the 35th Annual Meeting, Society of Nuclear Medicine, June 1988, San Francisco, CA.

TABLE 1
Results in 39 Patients with Thyroid Cancer Studied Postoperatively

Patients evaluated	50
²⁰¹ Tl SPECT imaging	42
No. with metastatic disease (all methods)	20/50 (40%)
¹³¹ I positive scans	12/19 (63%)
²⁰¹ Tl positive images	17/20 (85%)
Planar only	12/20 (60%)

RESULTS

The outcome of the study is summarized in Table 1. Of the 50 patients, 20 (40%) were found by all methods to have regional and/or distant metastases; in 12 of the patients with metastases the ¹³¹I scans were positive (63%). The planar ²⁰¹Tl images (not including cine views) were abnormal in 12 of the 20 patients (60%). In 5 additional patients (17/20), the SPECT images also were abnormal. Thus, the use of SPECT increased the sensitivity of lesion detectability with ²⁰¹Tl scanning by 25% (from 60% to 85%). However, in two patients with metastases, the ¹³¹I scans were positive and the SPECT images were negative so that reliance upon ²⁰¹Tl imaging alone would have missed the diagnosis.

Normal Findings

In the neck, the submaxillary glands were seen in all subjects, except after high-dose ¹³¹I therapy. Midline activity at the level of the base of the tongue was frequently identified in coronal views and is felt to represent lingual salivary glands (Fig. 1A). The thymus gland appeared as an inverted Y-shape in many individuals younger than 30 yr of age (Fig. 1B). In some subjects, the separate heads of the sternocleidomastoid muscle and the pharyngeal constrictor (Fig. 2) were seen. In the lungs, the pulmonary vasculature appeared

as a reticulated pattern, and branch points were often nodular, especially in coronal (Fig. 3) and transverse sectional images. The hepatic veins and the entrances of the superior and inferior vena cavae into the right atrium were identified in many subjects in coronal views (Fig. 3).

In general, cine images when displayed in rapid sequence were useful for orientation and for focusing attention on specific areas to be studied in greater detail on sectional reconstructions. Of the sectional images, coronal views were best for identifying abnormal foci and differentiating them from normal anatomic structures. Transverse sections of the chest were the most difficult to interpret.

Focal Abnormalities

In the neck and upper mediastinum, foci measuring 1.0 cm or larger on rectilinear (1:1) ¹³¹I scans were identifiable on coronal SPECT images, even when planar views were unremarkable (Figs. 4–5). In one patient, a palpable 1.0-cm anterior cervical node was not seen; when excised, this proved to be a cystic metastasis. In patients with discrete pulmonary metastases on chest roentgenogram or ¹³¹I scans, no focus smaller than 1.5 cm was seen on SPECT images which could be distinguished from normal vascular nodularity with certainty (Fig. 5).

Diffuse Abnormalities

Cine images when shown in motion picture format were useful in identifying diffuse micronodular pulmonary metastases in five patients. Anterior and posterior planar images were not as diagnostic as sectional reconstructions (Fig. 6). These patients all had significantly elevated serum thyroglobulin levels (>27 μ Iu/ml) as well as abnormal ¹³¹I scans (currently or in the past).

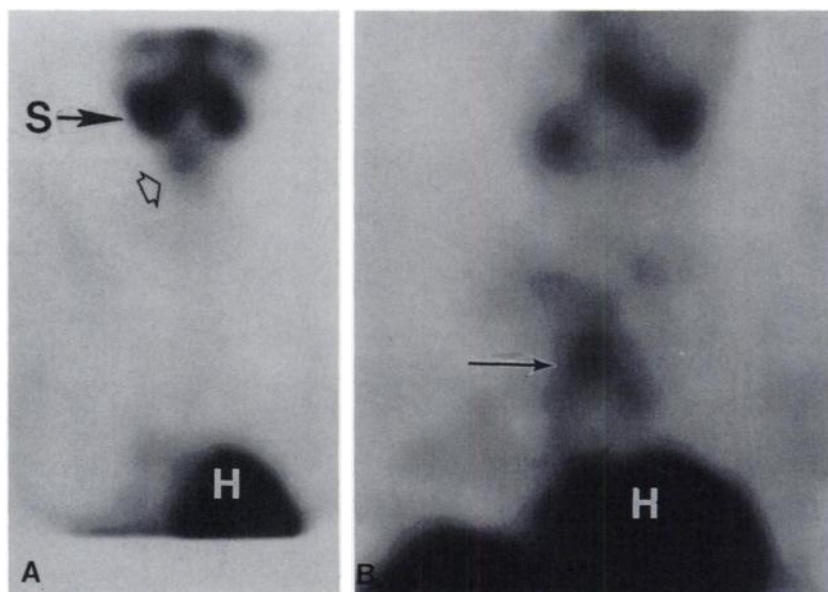


FIGURE 1
(A) Coronal image of neck and chest of a 31-yr-old woman, following total thyroidectomy for papillary carcinoma with no evidence of metastatic disease. Open arrow points to ²⁰¹Tl accumulation high in midline of neck at base of tongue (sublingual salivary tissue); S—submaxillary gland; H—heart. (B) Coronal ²⁰¹Tl sectional image through neck and anterior chest of a 31-yr-old woman with no evidence of metastatic disease (papillary carcinoma primary). The thymus gland appears as an inverted Y (arrow).

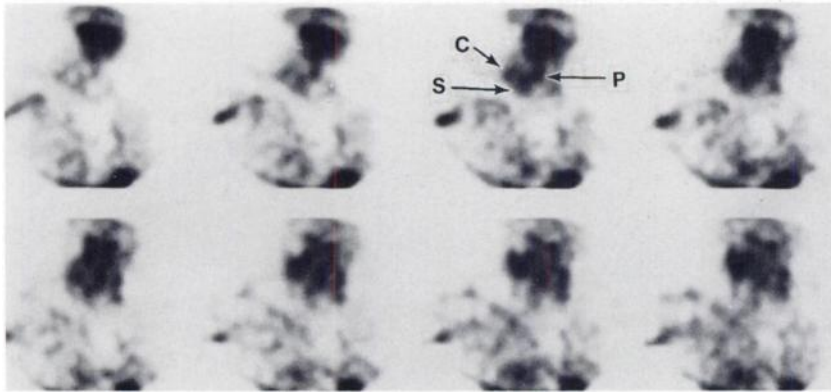


FIGURE 2

Sequential coronal ^{201}Tl images of neck and chest of a 64-yr-old woman who had undergone total thyroidectomy (but not radical neck dissection) and ^{131}I therapy for follicular carcinoma of thyroid. A recent 3-mCi ^{131}I scan of the neck showed no focal uptake, and subsequent autopsy revealed no residual disease in neck or chest. Note: sternal (S) and clavicular (C) heads of right sternocleidomastoid muscle and contralateral asymmetry (anatomic variant); M. constrictor pharyngis (P). Salivary glands visualize poorly because of prior ^{131}I therapy (625 mCi for lung and bone metastases).

False-Positive Findings

These findings are summarized in Table 2. In addition to the observations already noted, we found diffusely increased pulmonary uptake in some older patients, a number of whom had coronary artery disease. One patient had focal mediastinal uptake thought to be regionally metastatic breast cancer. The musculature of the back was often evident in cine imaging and sectional reconstructions.

DISCUSSION

We found that planar ^{201}Tl -chloride images detected thyroid cancer foci in 60% of patients with metastases, similar to results reported by many groups (range 35%–72%) (5,7,9,11). It might be argued that the yield could be improved by increasing the photon flux (greater dose, longer exposure time), increasing resolution (smaller camera closer to the neck, high-resolution parallel-hole



FIGURE 3

Sequential coronal ^{201}Tl images of neck and chest of a 70-yr-old man following thyroid lobectomy for follicular carcinoma and ^{131}I ablation of contralateral lobe. No metastases found by any method. Note reticular pattern of pulmonary vasculature, especially in lower lobes, and nodose configuration at branching points. Arrows point to location of orifices of superior and inferior vena cavae in right atrium.

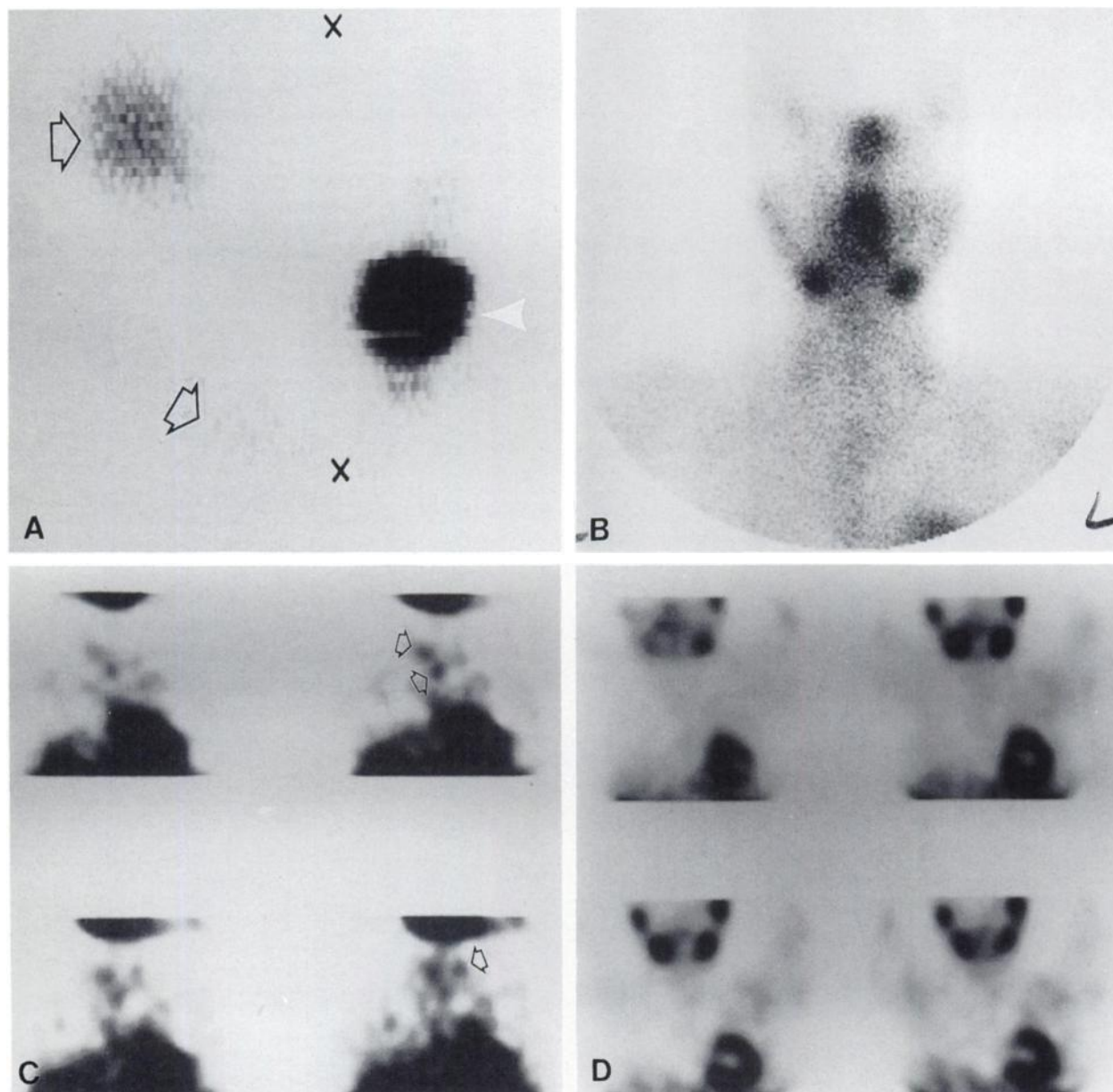


FIGURE 4

30-yr-old woman underwent near-total thyroidectomy for papillary carcinoma of right lobe with local extension. (A) Rectilinear scan of neck following 3.3-mCi ^{131}I shows tumor foci (arrows) and residual nubbins of left lobe (arrowheads). Upper X = mental protuberance; lower X = suprasternal notch. (B) Unremarkable ^{201}Tl planar image of head, neck, and upper chest. (C) Coronal ^{201}Tl SPECT image sequence shows metastatic foci in neck and residual left lobe nubbins (arrows), corresponding to ^{131}I scan. (D) Seven months following 102-mCi ^{131}I therapy dose, ^{201}Tl SPECT images in same coronal planes are now unremarkable, and the previously noted foci are gone.

or pinhole collimator), or taking multiple views of the neck and chest (posterior, oblique projections). Some groups that have reported a high percentage of positive results (range 82%–100%) have used special techniques such as a dual-headed camera fitted with high resolution collimators (10) or rectilinear scanning (which is a form of tomography) (12), but others have not (6). Furthermore, other investigators who have used similar tech-

niques to increase resolution have reported results not significantly different from ours (5,7,11).

We found that SPECT significantly improved the detectability of thyroid cancer metastases by ^{201}Tl -chloride, especially in the lower neck and upper mediastinum. Focal metastases, which were not seen on planar images or were visualized only vaguely or equivocally, were readily identified by SPECT. Coronal sections

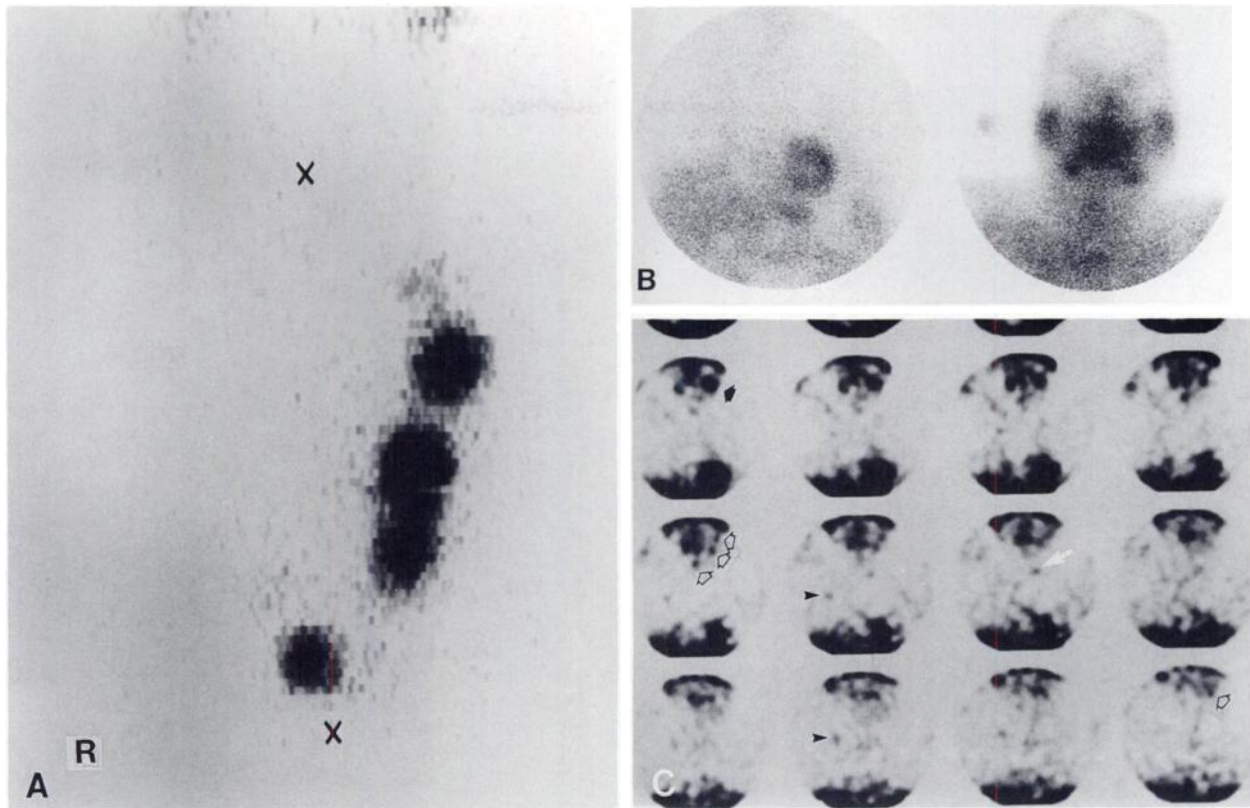


FIGURE 5
 43-yr-old man with papillary carcinoma of thyroid, metastatic to neck and lung. (A) Diagnostic (3.2 mCi) ^{131}I anterior rectilinear scan of neck showing multiple nodal metastases. Upper X = mental protuberance; lower X = suprasternal notch; R = right. (B) Unremarkable ^{201}Tl planar images of head, neck and upper chest. No metastases are visible. (C) Coronal ^{201}Tl images of neck and chest. Three of four neck nodes seen in the ^{131}I scan can be seen in one plane (open arrows) and the fourth in a deeper plane (open arrow). Submaxillary salivary gland (solid arrow). A left upper lobe metastasis noted on ^{131}I chest scan may not be the focus seen on the ^{201}Tl image (white arrow), since similar foci in the right lung (arrow heads) are undoubtedly vascular confluences, not lesions.

were best for this purpose. Some of these lesions were seen on ^{131}I scans. Foci in these locations as small as 1.0 cm were visualized, an improvement over planar imaging (6,9,13,14); many of the lesions were impalpable.

The ability of ^{201}Tl SPECT to detect multifocal pulmonary metastases visible on roentgenograms was not as good, although better than planar imaging. We were able to identify lesions larger than 1.5 cm, but not smaller ones, since normally branching vessels, especially in the right lower lobe, appear nodular on sectional images and cannot be distinguished from metastatic foci. Kusakabe and associates studied detectability of metastatic foci by ^{201}Tl -chloride planar imaging in relation to lesion size and reported that seven of eight metastatic sites in the lungs >2 cm were visible, but only one of five sites <2 cm (9) were visible. Nemce and associates reported false-negative ^{201}Tl rectilinear images in pulmonary foci previously treated with ^{131}I and presumably necrobiotic (12), but our patients with lung lesions smaller than 1.5 cm, which were undetect-

able by SPECT, also had larger, detectable lesions; none of them accumulated ^{131}I . This size may be the limitation of current methodology, since Tonami et al. have reported visualization of primary lung cancers larger than 1.5 cm using ^{201}Tl SPECT, but not smaller ones (18).

Disseminated micronodular pulmonary metastases (MPM), (extensive microscopic disease at or below the limit of radiographic detectability and chiefly affecting the lower lobes), were readily identified by SPECT, but planar images were vague and equivocal at best. Cine views in motion picture format were suggestive, although frequently only one or two of the 64 images showed the abnormality. The importance of MPM is illustrated by the finding that at least five of nine patients (55%) with lung lesions of thyroid carcinoma had MPM, documented by ^{201}Tl SPECT studies. These five patients, all of whom had elevated serum TG levels (>27 ng/ml) while on suppressive doses of thyroid hormone, represented 25% of all patients with metastases (5/20), a significant subset. In only two of these

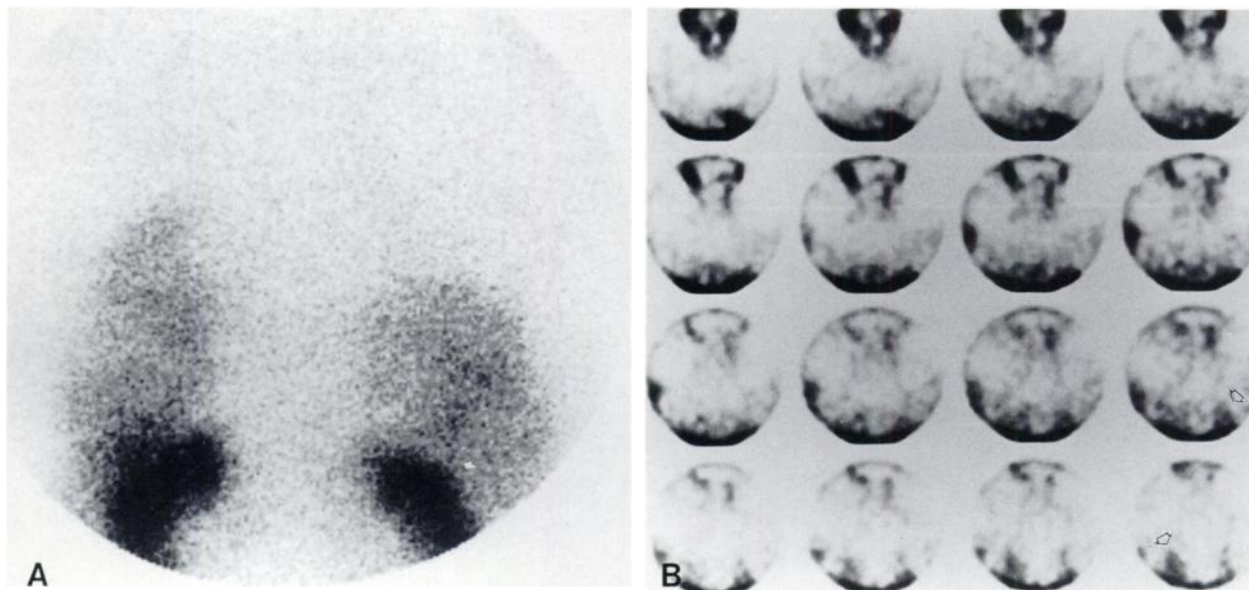


FIGURE 6

A 45-yr-old man who had been treated three times in the past with large doses of ^{131}I for disseminated micronodular pulmonary metastases. Most recent ^{131}I diagnostic scan (10 mCi) was interpreted as normal, but serum thyroglobulin was markedly elevated (81 ng/ml). Chest radiograph showed fibrotic pattern. (A) Posterior planar ^{201}Tl image is unremarkable. (B) Coronal sections of neck and chest posterior to heart show bilateral pulmonary infiltrates (arrows).

patients with MPM did the lesions appear to concentrate diagnostic scanning doses of ^{131}I (3–10 mCi), although three other patients had previously been treated with ^{131}I in doses >100 mCi with evidence of diffuse,

minimal to moderate uptake in the lungs. Recently, Pacini and associates reported on 10 patients with elevated serum TG levels and normal chest radiographs in a group of 135 consecutive postoperative patients with thyroid cancer (7.4%), who had pulmonary metastases visible following therapeutic doses of ^{131}I but not diagnostic doses (19). Schlumberger et al. have reported similar findings (20). Thus, it would appear that in postoperative patients with elevated serum TG and no evidence of focal metastatic disease on chest radiographs, ^{201}Tl SPECT may be able to detect both regional disease in the neck and disseminated micronodular disease in the lungs not seen on ^{201}Tl planar images but identifiable following administration of therapeutic doses (>100 mCi) of radioiodine ^{131}I .

Although ^{201}Tl planar imaging has been recommended for routine follow-up of thyroid cancer patients (6,10,17), and even as a replacement for ^{131}I scanning, our findings do not support this position. Thallium-201 SPECT imaging, however, appears to be extremely useful, particularly in the detection of regional disease in the neck and disseminated micronodular pulmonary metastases. Probably all postoperative patients with this disorder deserve at least one ^{201}Tl SPECT imaging study of the neck and chest for staging purposes, in addition to ^{131}I scanning and chest radiograph. An abnormal ^{201}Tl SPECT study in a postoperative cancer patient can direct attention to focal metastatic disease possibly amenable to ^{131}I therapy, surgery (10,13,21,22), or external-beam radiotherapy (10), but uptake is nonspecific (2), and metastatic foci smaller than 1.0 cm in the neck or 1.5 cm in the lungs have not been detectable.

TABLE 2
False-Positive and False-Negative ^{201}Tl SPECT Images
for Thyroid Cancer

False-Positive Images

Neck

1. Lingual midline salivary glands
2. Normal musculature (heads of sternocleidomastoid muscle; pharyngeal constrictor)
3. Postoperative changes (excised submaxillary glands, sternomastoid muscle)
4. ^{131}I post-therapy (asymmetric submaxillary gland activity)

Lung

1. Thymus gland
2. Normal vascular branching (nodular)
3. Orifices of vena cavae
4. Other vascular uptake (especially in transverse sections)
5. Nonthyroidal cancer (primary or metastatic)
6. Hiatal hernia
7. Age over 50 (diffuse lung uptake)
8. Coronary artery disease (diffuse lung uptake)
9. Normal musculature (latissimus dorsi; erector spinae)

False-Negative Images

Neck

1. Size <1 cm
2. Cystic metastases

Lung

1. Size <1.5 cm
2. ^{131}I post-therapy necrobiosis (12)

Thallium-201 SPECT appears to have an important role in the staging of thyroid cancer, but the details of that role remain to be defined.

ACKNOWLEDGMENTS

The authors wish to express their appreciation to the staff technologists who performed the studies, and to Ms. Ola McCrea for typing the manuscript.

Presented in part at the 35th Annual Meeting, Society of Nuclear Medicine, San Francisco, June 14–17, 1988.

REFERENCES

1. Tonami N, Bunko H, Michigishi T, Kuwajima A, Hisada K. ^{201}Tl scintigraphy in patients with cold thyroid nodules. *Clin Nucl Med* 1978; 3:217–221.
2. Hisada K, Tonami N, Miyamae T, et al. Clinical evaluation of tumor imaging with ^{201}Tl chloride. *Radiology* 1978; 129: 497–500.
3. Eguchi S, Matsumura T, Nomura Y, Yanagita T. Thyroid scanning with ^{201}Tl chloride. *Otologia (Fukuoka)* 1978; 24: 353–359.
4. Palermo F, Bruniera F, Caldato L, Siega MD, Lazzarini M, Mareso A. Scintigraphic evaluation of the “cold” thyroid areas. *Eur J Nucl Med* 1979; 4:43–48.
5. Harada T, Ito Y, Shimaoka K, Taniguchi T, Matsudo A, Senoo T. ^{201}Tl chloride scan for thyroid nodule. *Eur J Nucl Med* 1980; 5:125–130.
6. Makimoto K, Ohmura M, Tamada A, et al. Combined scintiscans in the diagnosis of thyroid carcinomas. *Acta Otolaryngol (Stockh)* 1985; 410(suppl):189–194.
7. Ikekubo K, Higa T, Hirasa M, Ishihara T, Waseda N, Mori T. Imaging and echography in the diagnosis of thyroid nodules. *Clin Nucl Med* 1986; 11:145–149.
8. Varma V, Reba R. Comparative study of Tl-201 and I-131 scintigraphy in postoperative metastatic thyroid carcinoma. In: Raynard C, ed. *Nuclear medicine and biology. Proceedings 3rd world congress of nuclear medicine and biology, Vol. 1*. Paris: Pergamon Press, 1982:103–104.
9. Kusakabe K, Inoue Y, Kawasaki Y, et al. Usefulness of Tl-201 chloride and Na I-123 scintigraphy in detection of metastasis from thyroid carcinoma. *Kaku Igaku* 1984; 21:941–951.
10. Hoefnagel CA, Delprat CC, Marcuse HR, de Vijlder JJM. Role of thallium-201 in total-body scintigraphy in follow-up of thyroid carcinoma. *J Nucl Med* 1986; 27:1854–1857.
11. Brendel JJ, Gugot M, Jeandot R, Lefort G, Manciet G. Follow-up of differentiated thyroid carcinoma. *J Nucl Med* 1988; 29:1515–1520.
12. Némec J, Zamrazil V, Pohunkova D, Rohling S, Holub V. ^{201}Tl scintigraphy in the evaluation of differentiated thyroid cancer. *Eur J Nucl Med* 1984; 9:261–264.
13. Fukuchi M, Tachibana K, Kuwata K, et al. Thallium-201 imaging in thyroid carcinoma—appearance of a lymph node. *J Nucl Med* 1978; 19:195–196.
14. Tonami N, Hisada. ^{201}Tl scintigraphy in postoperative detection of thyroid cancer: a comparative study with ^{131}I . *Radiology* 1980; 136:461–464.
15. Tennvall J, Palmer J, Cederquist E, et al. Scintigraphic evaluation and dynamic studies with thallium-201 in thyroid lesions with suspected cancer. *Eur J Nucl Med* 1981; 6:295–300.
16. Piers DA, Sluiter WJ, Willemse PHB, Doórenbos H. Scintigraphy with ^{201}Tl for detection of thyroid cancer metastases. *Eur J Nucl Med* 1982; 7:515–517.
17. Müller-Brand J, Fridrich R, Spicher E, Staub JJ. Thyreoglobulin als tumormarker und thalliumszintigraphie zur verlaufskontrolle beim differenzierten schilddrusenkarzinom [Abstract]. *Schweiz Med Wochenschr* 1983; 113:325–327.
18. Tonami N, Shuke N, Yokoyama K, et al. Thallium-201 single photon emission computed tomography in the evaluation of suspected lung cancer. *J Nucl Med* 1989; 30:997–1004.
19. Pacini FL, Lippi F, Formica N, et al. Therapeutic doses of iodine-131 revealed undiagnosed metastases in thyroid cancer patients with detectable serum thyroglobulin levels. *J Nucl Med* 1987; 28:1888–1891.
20. Schlumberger M, Arcangioli O, Piekarski JD, Tubiana M, Parmentier C. Detection and treatment of differentiated thyroid carcinoma in patients with normal chest x-rays. *J Nucl Med* 1988; 29:1790–1794.
21. Cosimelli M, Schillaci A, Benaglia T. Diagnosing metastases of differentiated thyroid carcinoma with thallium-201 scan: a case report. *Clin Oncol* 1984; 10:163–166.
22. Arnstein NB, Juni JE, Sisson JC, Lloyd RV, Thompson NW. Recurrent medullary carcinoma of the thyroid demonstrated by thallium-201 scintigraphy. *J Nucl Med* 1986; 27:1564–1568.